

Riemannian Optimization on the Oblique Manifold for Sparse Simplex Constraints via Multiplicative Updates

Flavia Esposito^{1*} and Andersen Ang²

¹Department of Mathematics, University of Bari Aldo Moro, Bari, 70125, Italy.

²School of Electronics and Computer Science, University of Southampton, Southampton, SO17 1BJ, United Kingdom.

*Corresponding author(s). E-mail(s): flavia.esposito@uniba.it;
Contributing authors: andersen.ang@soton.ac.uk;

Abstract

Low-rank optimization problems with sparse simplex constraints involve variables that must satisfy nonnegativity, sparsity, and sum-to-one conditions, making their optimization particularly challenging due to the interplay between low-rank structures and constraints. These problems arise in various applications, including machine learning, signal processing, environmental fields, and computational biology. In this paper, we propose a novel manifold optimization approach to tackle these problems efficiently. Our method leverages the geometry of oblique rotation manifolds to reformulate the problem and introduces a new Riemannian optimization method based on Riemannian gradient descent that strictly maintains the simplex constraints. By exploiting the underlying manifold structure, our approach improves optimization efficiency. Experiments on synthetic datasets compared to standard Euclidean and Riemannian methods show the effectiveness of the proposed method.

Keywords: manifold, optimization, simplex, nonnegativity, sparsity

MSC Classification: 15A23 , 65K10 , 49Q99 , 90C26 , 90C30

1 Introduction

Low-rank decomposition such as Nonnegative Matrix Factorization (NMF) exploits the fact that high-dimensional matrices can be well-approximated by a sum of rank-one components [1]. This reduces the computational complexity of the operations in the optimization while preserving the essential structure of the data [2]. In NMF, the goal is to approximate a nonnegative matrix $\mathbf{X} \in \mathbb{R}_+^{m \times n}$ as the product of two low-rank matrices $\mathbf{W} \in \mathbb{R}_+^{m \times r}$ and $\mathbf{H} \in \mathbb{R}_+^{r \times n}$, where $r \leq \min(m, n)$. Mostly, additional constraints — such as sparsity, smoothness, or low total variation — can be imposed to enhance interpretability and performance. In this paper, we focus on combining three conditions: **nonnegativity**, **sparsity**, and **sum-to-one normalization**, useful in practical applications¹. We consider the following optimization problem that we call NSSls (Nonconvex-sparse simplex least squares)

$$\operatorname{argmin}_{\mathbf{H}} \frac{1}{2} \|\mathbf{X} - \mathbf{W}\mathbf{H}\|_F^2 + \lambda \|\mathbf{H}\|_{1/2}^{1/2} \quad \text{s.t.} \quad \underbrace{\mathbf{H} \geq \mathbf{0}, \mathbf{H}^\top \mathbf{1}_r = \mathbf{1}_n}_{\text{columns of } \mathbf{H} \text{ in unit simplex}}, \quad (\text{NSSls})$$

where $\|\cdot\|_F$ is the Frobenius norm, $\lambda \in \mathbb{R}$ is a penalty hyperparameter, $\mathbf{1}_r$ is vector-of-1 in \mathbb{R}^r , and the nonconvex $\ell_{1/2}^{1/2}$ -quasi-norm [4], for promoting sparsity², is defined as

$$\|\mathbf{H}\|_{1/2}^{1/2} = \sum_{i=1}^r \sum_{j=1}^n \sqrt{H_{ij}}. \quad (\ell_{1/2}^{1/2}-\text{quasi-norm})$$

Model (NSSls) encourages the columns in \mathbf{H} to be concentrated in the boundary of a simplex, which promotes sparsity, nonnegativity and normalization. See Fig. 1.

Contribution In this letter, we introduce a novel approach to for solving (NSSls) using a Riemannian optimization algorithm [5]. This new method, called Riemannian Multiplicative Update (RMU), is based on Riemannian gradient descent and maintains the smoothness condition on the manifold. The main advantage of RMU is computational efficiency on handling the simplex constraint: RMU solves (NSSls) by incorporating the constraint directly into the minimization process. This is different from existing works [6–8], we put the details in Section 3.

Paper Organization Section 2 presents the manifold formalization of (NSSls), reviews and describes manifold optimization for solving it. Section 3 presents a brief experimentation, while Section 4 concludes the paper.

Remark 1 (Nonconvex simplex) *The simplex constraint in (NSSls) is a nonconvex set for each column of \mathbf{H} . This nonconvex set introduces complication for zero vectors. We remark that all columns of \mathbf{H} in the experiment and algorithm are not zero vector.*

¹For example, in biomedicine, \mathbf{X} represents gene expression levels in data, and \mathbf{H} quantifies the relative abundance of metagenes in each sample [3]. In remote sensing, \mathbf{X} represents spectral signatures in data, and the sum-to-one constraint ensures physically meaningful interpretations by computing the fractional abundance of endmember materials [1].

² $\ell_{1/2}$ is ℓ_p -norm with $p = 1/2$. Such a norm is not a norm because it is not homogeneous.

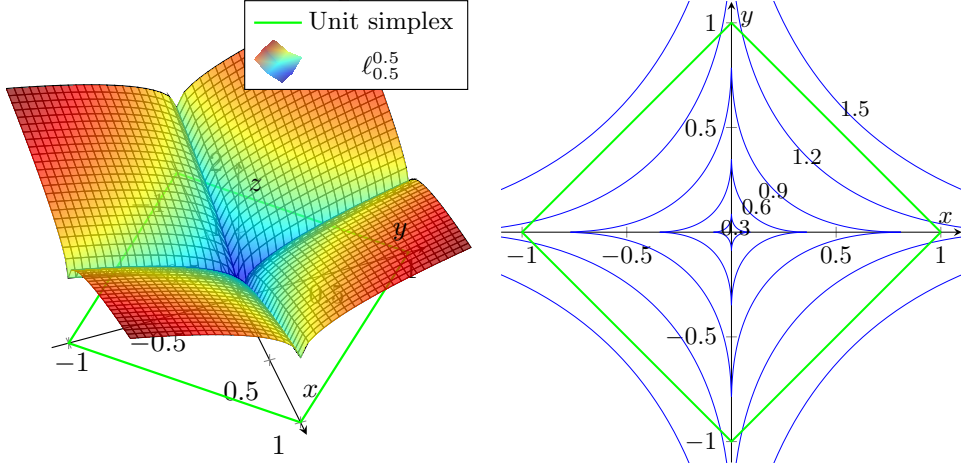


Fig. 1: The plot of the (nonconvex) $\ell_{0.5}^{0.5}$ –quasi-norm and the simplex constraint. Left: the surface of $\ell_{0.5}^{0.5}$ –quasi-norm in \mathbb{R}^2 and the simplex constraint (in green). Right: the level set plot. Minimizing the $\ell_{0.5}^{0.5}$ –quasi-norm on the green simplex gives the solution sitting on the corner of the simplex, leading to sparsity.

2 Manifold formulation

In the literature there are some approaches to solving constraints and penalization similar to (NSSIs) [6–8]. However, some of these methods are Euclidean and enforce the constraints with a post-normalization step in the algorithm. On the contrary, in this paper, we rewrite (NSSIs) using Riemannian optimization theory of the oblique rotation manifold to directly include the constraint in the optimization process. We remark also that even if the other Riemannian method follows a similar formulation of the problem, it needs several steps and more computational iteration costs than the proposed method, as we will observe in Section 3.

2.1 Formulation in oblique rotation manifold

Following [7], we reformulate the sum-to-one constraints in (NSSIs) by introducing a rectangular matrix $\mathbf{A} \in \mathbb{R}^{r \times n}$. We consider \mathbf{H} as $\mathbf{H} = \mathbf{A} \odot \mathbf{A}$, where \odot is Hadamard product, and we embed \mathbf{A} in the rank- r oblique rotation manifold [9, page 14]:

$$\mathcal{OB}(r, n) = \{\mathbf{A} \in \mathbb{R}^{r \times n} \mid \text{diag}(\mathbf{A}^\top \mathbf{A}) = \mathbf{I}_n\}, \quad (1)$$

where $\text{diag} : \mathbb{R}^{n \times n} \rightarrow \mathbb{R}^{n \times n}$ takes the diagonal elements of the input matrix to form a diagonal matrix, and \mathbf{I}_n is the identity matrix.

Following [7, Section III A] , we have the following lemma.

Lemma 1 *The matrix \mathbf{H} stays in the simplex if and only if $\mathbf{H} = \mathbf{A} \odot \mathbf{A}$ with $\mathbf{A} \in \mathcal{OB}(r, n)$.*

Proof The nonnegativity is given by the definition of $\mathbf{H} = \mathbf{A} \odot \mathbf{A}$, i.e., we have $H_{ij} = A_{ij}^2 \geq 0$. The sum-to-one constraint also naturally follows, since:

$$\sum_{i=1}^r H_{ij} = \sum_{i=1}^r A_{ij}^2 = (\mathbf{A}^\top \mathbf{A})_{jj} \stackrel{\mathbf{A} \in \mathcal{OB}(r,n)}{=} 1, \quad \text{for all } j. \quad \square$$

Based on Lemma 1, we rewrite (NSSls) in a manifold optimization formulation that aims to minimize a new function $f : \mathbb{R}^{r \times n} \rightarrow \mathbb{R}^{r \times n}$, which we call the problem L1-quartic-ls (L1-quartic least squares)

$$\operatorname{argmin}_{\mathbf{A} \in \mathcal{OB}(r,n)} \left\{ f(\mathbf{A}) = \frac{1}{4} \|\mathbf{X} - \mathbf{W}(\mathbf{A} \odot \mathbf{A})\|_F^2 + \lambda \|\mathbf{A}\|_1 \right\}, \quad (\text{L1-quartic-ls})$$

where $\|\mathbf{A}\|_1 = \sum_{ij} |A_{ij}|$ is the entry-wise ℓ_1 norm of \mathbf{A} due to $(x^{\frac{1}{2}})^2 = |x|$.

Remark 2 (Why $\ell_{1/2}^{1/2}$ -quasi-norm.) *Other nonconvex sparsity-inducing norms such as the ℓ_1 - ℓ_2 [10] are also available. In this work we use the nonconvex $\ell_{1/2}^{1/2}$ -quasi-norm due to Lemma 1: from $\mathbf{H} = \mathbf{A} \odot \mathbf{A}$, the Hadamard product cancels with the $1/2$ -power in the $\ell_{1/2}^{1/2}$ -quasi-norm.*

Remark 3 (Nonconvexity of the objective functions) *Both the objective functions in (NSSls) and (L1-quartic-ls) are nonconvex. In (NSSls), the term $\ell_{1/2}^{1/2}$ -quasi-norm is nonconvex. In (L1-quartic-ls), the term $\|\mathbf{X} - \mathbf{W}(\mathbf{A} \odot \mathbf{A})\|_F^2$ is quartic in \mathbf{A} and is generally nonconvex [11].*

Considering the new formulation (L1-quartic-ls) in a manifold optimization problem, and the fact that the solution of (L1-quartic-ls) solves (NSSls), by Lemma 1, in the following we review some concepts from Riemannian optimization to solve (L1-quartic-ls). We would like to note that we keep the material minimum, but for details, we refer to [7, 9, 12].

2.2 Oblique rotation matrices manifold

The oblique rotation manifold in (1) is an embedded submanifold of $\mathbb{R}^{r \times n}$. We want to observe that: first $\mathcal{OB}(r, n)$ can be seen as the product of r spheres, where each sphere is $\mathcal{S}^{n-1} = \{\mathbf{x} \in \mathbb{R}^n \mid \|\mathbf{x}\|_2 = 1\}$; second, that $\mathcal{OB}(r, n)$ can also be seen as a relaxed version of Stiefel manifold $\mathcal{ST}(r, n) = \{\mathbf{A} \in \mathbb{R}^{r \times n} \mid \mathbf{A}^\top \mathbf{A} = \mathbf{I}_n\}$.

Performing Riemannian optimization requires the notion of the tangent space of $\mathcal{OB}(r, n)$ at a point \mathbf{A} , denoted as $\mathcal{T}_{\mathbf{A}} \mathcal{OB}(r, n)$,

$$\mathcal{T}_{\mathbf{A}} \mathcal{OB}(r, n) = \{\mathbf{Z} \in \mathbb{R}^{r \times n} \mid \operatorname{diag}(\mathbf{A}^\top \mathbf{Z}) = \mathbf{0}\},$$

whereas the associated null space is defined as:

$$\mathcal{N}_{\mathbf{A}} \mathcal{OB}(r, n) = \{\mathbf{A} \mathbf{D} \mid \mathbf{D} \in \mathbb{R}^{n \times n} \text{ is diagonal}\}.$$

The projectors over these spaces at \mathbf{A} for a generic matrix $\mathbf{Z} \in \mathbb{R}^{r \times n}$ are defined as:

$$\mathcal{P}_{\mathcal{N}_{\mathbf{A}}}(\mathbf{Z}) = \mathbf{A} \text{diag}(\mathbf{A}^{\top} \mathbf{Z}), \quad \mathcal{P}_{\mathcal{T}_{\mathbf{A}}}(\mathbf{Z}) = \mathbf{Z} - \mathbf{A} \text{diag}(\mathbf{A}^{\top} \mathbf{Z}), \quad (2)$$

and will be essential to derive the formulation of the Riemannian gradient for our method. To conclude, we need a function to move a point back to the manifold, defined as the metric retraction:

$$\mathcal{R}_{\mathbf{A}}(\mathbf{Z}) = (\mathbf{A} + \mathbf{Z}) \left(\text{diag}((\mathbf{A} + \mathbf{Z})^{\top} (\mathbf{A} + \mathbf{Z}))^{-1/2} \right). \quad (3)$$

Before deriving the new RMU for problem (L1-quartic-ls), we recall the RMU proposed in [5].

2.3 Riemannian Multiplicative Update

Considering a general nonnegative problem $\underset{\mathbf{x} \in \mathcal{M}}{\text{argmin}} f(\mathbf{x})$, with $\mathbf{x} \geq 0$, RMU is a method proposed in [5] based on Riemannian gradient descent [12].

For a manifold \mathcal{M} , the proposed method make uses: i) Riemannian gradient $\text{grad}f$, ii) a metric retraction $\mathcal{R}(\cdot)$, iii) and an appropriate step-size α .

Theorem 1 ([5]) *Denote $\mathbf{v}_k = -\text{grad}f(\mathbf{x}_k)$ the anti-parallel direction of the Riemannian gradient of a manifold \mathcal{M} at \mathbf{x}_k , and let $\mathcal{R}_{\mathbf{x}_k}$ be the metric retraction onto \mathcal{M} . If a nonnegative \mathbf{x}_k is updated by $\mathbf{x}_{k+1} = \mathcal{R}_{\mathbf{x}_k}(\alpha \odot \mathbf{v}_k)$ with an element-wise stepsize $\alpha = \mathbf{x}_k \oslash \text{grad}^+ f(\mathbf{x}_k) \in E$, then $\mathbf{x}_{k+1} \geq \mathbf{0}$ and is on \mathcal{M} .*

We would like to note that RMU is not strictly a Riemannian gradient descent method, since the element-wise operations as linear transformations in general do not preserve the tangent condition of a manifold at a point. This phenomenon may contribute to a slower convergence rate, a tendency that was clearly reflected in the outcomes of our experimental analysis in Section 3.

We are now ready to move on to the explicit update of \mathbf{A} .

2.4 Algorithm for minimizing (L1-quartic-ls) over $\mathcal{OB}(r, n)$

By Theorem 1, the update $\mathbf{A}^{k+1} = \mathcal{R}_{\mathbf{A}^k}(-\alpha \odot \text{grad}f(\mathbf{A}^k))$ converges to a stationary point of function (L1-quartic-ls) for $\mathbf{A} \in \mathcal{OB}(r, n)$. In this update, function $\mathcal{R}(\cdot)$ is the retraction (3), and $\text{grad}f(\cdot)$ is the Riemannian gradient computed with the orthogonal projector over the tangent space in (2) over the Euclidean (sub-)gradient:

$$\nabla f(\mathbf{A}) = -2\mathbf{W}^{\top}(\mathbf{X} - \mathbf{W}(\mathbf{A} \odot \mathbf{A})) \odot \mathbf{A} + \lambda' \text{sign}(\mathbf{A}),$$

where sign is the element-wise sign function (subgradient of the ℓ_1 -norm) with $\text{sign}(x) = 1$ if $x > 0$ and $\text{sign}(x) = -1$ if $x < 0$ and $\text{sign}(x) \in [-1, 1]$ if $x = 0$, see for details [13, Example 3.4]. The symbol λ' is a re-scaled λ (with respect to the $1/4$ in f when taking the derivative).

Let $\mathbf{Q} = \mathbf{W}^\top \mathbf{W}$ and $\mathbf{P} = \mathbf{W}^\top \mathbf{X}$, the Riemannian (sub-)gradient is defined as:

$$\begin{aligned} \text{grad}f(\mathbf{A}) &= \underbrace{\left(\mathbf{Q}(\mathbf{A} \odot \mathbf{A}) \right) \odot \mathbf{A} + \mathbf{A} \text{diag} \left[\mathbf{A}^\top (\mathbf{P} \odot \mathbf{A}) \right] + \lambda' \text{sign}(\mathbf{A})}_{\text{grad}^+ f} \\ &\quad - \underbrace{\left\{ \mathbf{P} \odot \mathbf{A} + \mathbf{A} \text{diag} \left[\mathbf{A}^\top \left(\mathbf{Q}(\mathbf{A} \odot \mathbf{A}) \right) \odot \mathbf{A} \right] + \lambda' \mathbf{A} \text{diag} \left[\mathbf{A}^\top \text{sign}(\mathbf{A}) \right] \right\}}_{\text{grad}^- f}, \end{aligned}$$

where we performed a sign-wise splitting

$$\text{grad}f(\mathbf{A}) = \text{grad}^+ f(\mathbf{A}) - \text{grad}^- f(\mathbf{A}).$$

Then, from Theorem 1, the RMU update is:

$$\begin{aligned} \mathbf{B}^k &= \mathbf{A}^k \odot \text{grad}^- f(\mathbf{A}^k) \oslash \text{grad}^+ f(\mathbf{A}^k), \\ \mathbf{A}^{k+1} &= \mathbf{B}^k \oslash \text{diag}[(\mathbf{B}^k)^\top \mathbf{B}^k]^{-1/2}, \end{aligned}$$

where \oslash is element-wise division.

Finally, after we find the value of \mathbf{A} , we compute $\mathbf{H} = \mathbf{A} \odot \mathbf{A}$.

Remark 4 (Subgradient) *Riemannian gradient method usually applies to differentiable function. However, in (L1-quartic-ls), f contains $\|\cdot\|_1$ that is a possibly nondifferentiable. The subgradient of $\|\cdot\|_1$, denoted as $\partial\|\mathbf{A}\|_1$, has the form*

$$\partial\|\mathbf{A}\|_1 = \text{sign}(\mathbf{A}) = \left\{ \mathbf{G} \in \mathbb{R}^{r \times n} : G_{ij} \in \begin{cases} \{0\} & \text{if } A_{ij} \neq 0 \\ [-1, 1] & \text{if } A_{ij} = 0 \end{cases} \right\}.$$

Moreover, we remark that the structure $\text{sign}(\mathbf{A}) - \mathbf{A} \text{diag}[\mathbf{A}^\top \text{sign}(\mathbf{A})]$ comes from the projectors in (2) applied on $\partial\|\mathbf{A}\|_1$.

3 Numerical Experiments

In this section, we show numerical results of RMU compared with other methods and tested on different synthetic datasets.

3.1 Comparative methods

We compare RMU with three methods: one based on Riemannian optimization and two from standard Euclidean optimization.

- **Riemannian method:** The work [7] proposed a Riemannian Conjugate Method (RCG) for solving (NSSls). In addition to the Riemannian gradient, RCG also computes: i) a conjugate direction, a hybrid (Dai-Yuan and Hestenes-Stiefel) stepsize using vector transport, iii) update stepsize using Wolfe line search (with at most 5 iterations, following [1]).

- **Euclidean-based methods.** We also consider two Euclidean-based approaches.
 - **EMU-proj heuristic:** For Problem (NSSls) without the sum-to-1 constraint, the following update formula for \mathbf{H} is proposed by [6]

$$\mathbf{H}_{k+1}^{\text{EMU}} = \mathbf{H}_k \odot \left(\mathbf{W}^\top \mathbf{M} \oslash \left(\mathbf{W}^\top \mathbf{W} \mathbf{H}_k \oplus \frac{\lambda}{2} \sum_{ij} \sqrt{H_{ij}} \right) \right), \quad (\text{EMU})$$

which is a modified version of the work by Hoyer [14], where \oplus is element-wise addition. To solve Problem (NSSls) by EMU, we consider the heuristic

$$\mathbf{H}_{k+1} = \text{proj}_\Delta \left[\mathbf{H}_{k+1}^{\text{EMU}} \right], \quad (\text{EMU-proj})$$

where proj_Δ is the column-wise projection onto the unit-simplex. Given a matrix $\mathbf{X} = [\mathbf{x}_1, \dots, \mathbf{x}_n]$ with n columns, then $\text{proj}_\Delta(\mathbf{X})$ replaces each \mathbf{x}_i by $\mathbf{x}_i / \|\mathbf{x}_i\|_1$.

- **SparseMU-proj heuristic:** The sparse multiplicative update proposed by [15] has a form similar to EMU

$$\mathbf{H}_{k+1}^{\text{SMU-L1}} = \mathbf{H}_k \odot \left(\mathbf{W}^\top \mathbf{M} \oslash \mathbf{W}^\top \mathbf{W} \mathbf{H}_k \oplus \lambda \right), \quad (\text{SMU-L1})$$

which minimizes a different objective function from the one in (NSSls), as

$$\underset{\mathbf{H} \geq 0}{\text{argmin}} \frac{1}{2} \|\mathbf{X} - \mathbf{W} \mathbf{H}\|_F^2 + \lambda \|\mathbf{H}\|_1.$$

We also remark that the difference between EMU and SMU-L1 is on the regularization parameter, where the latter uses a constant value of λ , while the former adopts a dynamically changing λ scaled by $\sum \sqrt{H_{ij}}$. To solve Problem (NSSls) by SMU-L1, we consider the heuristic with the same projection of EMU-proj:

$$\mathbf{H}_{k+1} = \text{proj}_\Delta \left[\mathbf{H}_{k+1}^{\text{SMU-L1}} \right]. \quad (\text{SparseMU-proj})$$

We emphasize that SparseMU-proj is not designed to solve NSSLa, however we still plot in our experiment for comparisons due to its proximity to our problem.

Remark 5 We also considered Sparse Coding [15] for comparisons. However, preliminary tests showed that the method consistently performed the worst and was therefore discarded.

Table 1 shows the per-iteration computational cost of the methods. In the Riemannian framework, compared with RCG, the RMU approach has a lower per-iteration cost.

Table 1: Per-Iteration complexities

Operation	EMU-proj	SMU-L1	RMU	RCG
Elementwise \sqrt{H}	rn	—	rn	rn
Column sums $\sum \sqrt{H}$	$rn - 1$	—	—	—
Sign computation	—	—	rn	—
Matrix mult. $W^T W H$	$(2r^2 - r)n$	$(2r^2 - r)n$	$(2r^2 - r)n$	$(2r^2 - r)n$
Diagonal operations	—	—	$6rn$	—
Elementwise operations	$4rn$	$4rn$	$10rn$	$8rn$
Riemannian gradient	—	—	$4rn$	$(4r^2 + 6r)n$
Retraction	—	—	$3rn$	$5rn$
Vector transport	—	—	—	$4rn$
Wolfe line search	—	—	—	$(10r^2 + 50r)n$
Projection (normalization)	$(3r - 1)n$	$(3r - 1)n$	—	—
Total FLOPs	$(2r^2 + 8r - 1)n$	$(2r^2 + 6r - 1)n$	$(2r^2 + 24r)n$	$(16r^2 + 74r)n$

3.2 Experimental settings

We generate a matrix \mathbf{X} as the product of two low-rank matrices $\mathbf{W}_{\text{true}}, \mathbf{H}_{\text{true}}$ such as $\mathbf{X} = \mathbf{W}_{\text{true}} \mathbf{H}_{\text{true}} + \sigma \mathbf{E}$. Both matrices $\mathbf{W}_{\text{true}}, \mathbf{H}_{\text{true}}$ are generated by sampling uniform distribution, where \mathbf{H}_{true} is controlled to only have $s\%$ non-zero entries. The matrix \mathbf{E} is a noise matrix following uniform distribution, with $\sigma \in \mathbb{R}$ as scaling factor. We perform 100 Monte Carlo runs of the algorithms according to the randomness of the dataset generation.

All the algorithms start with the same initialization and penalty parameter λ . We initialize the algorithms by NNSVD [16]. Given an initial variable H_{ini} , we select the parameter λ as the ratio $0.5\|\mathbf{X} - \mathbf{W}H_{\text{ini}}\|_F^2/\|\mathbf{H}_{\text{ini}}\|_{1/2}^{1/2}$, which balances the least squares part and the sparsity part at the beginning of the optimization process.

We stop the algorithms if either it reaches the maximum number of iteration k_{max} or the maximum runtime T_{max} . The experiments are conducted in MATLAB 2023a in a machine with OS Windows 11 Pro on a AMD Ryzen 7 7700 8-Core Processor CPU 3.80 GHz and 64GB RAM.

3.3 Evaluation metrics

Since the four methods have different per-iteration complexity, plotting the objective function value F versus iteration k nor versus time t provide a complete and fair comparison of the algorithm. See Fig. 2 for an example.

For each method we report the mean and standard deviation of the objective function, a ranking based on the area under curve (AUC) metric, and a median sparsity measure of \mathbf{H} .

AUC metric: The ranking based on the AUC metric is computed over 100 MC runs. The i th entry of the ranking vector indicates the number of times the algorithm generated the i th best solution. In fact, running each algorithm with the same initialization and modelling parameters, we obtain four sequences in the form of $\{t_k, F_k\}_{k \in \mathbb{N}}$, where F_k is the objective function value F at the k th iteration, and t_k is the time at the

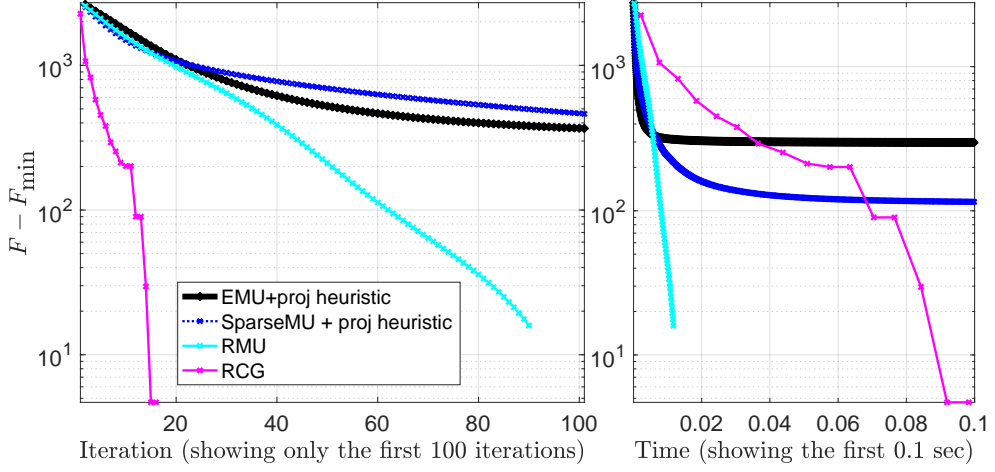


Fig. 2: A typical convergence plot of the four methods. Here in terms of iterations, the convergence of RCG has the best performance, however, it takes the highest amount of computational time for performing one iteration (shown by a larger gap between two consecutive points on the right).

k th iteration. To handle the issue of having different per-iteration cost across different methods, we use AUC as a measurement to compare the performance. Considering the computational runtime $t = 0$ to the time $t = T_{\max}$, AUC is defined by

$$\text{AUC} = \int_0^{T_{\max}} F(t) dt,$$

where the integral represents the total accumulated $F(t)$ over time. For minimization, a smaller integral means the algorithm kept the error low for most of the time. Numerically, we treat $F(t)$ as a continuous function by interpolating between the points $\{t_k, F_k\}_{k \in \mathbb{N}}$, then the trapezoidal rule estimates the area between them as $\Delta_k = \frac{1}{2}(F_{k-1} + F_k)(t_k - t_{k-1})$. Hence the AUC of a method is the sum of all the Δ_k .

We decided to work with AUC since:

- It ignores the number of iterations k and focuses on real time t , making it fair to compare algorithms with varying iteration counts.
- The per-iteration costs are embedded in t_k , so costly iterations are only rewarded if they significantly reduce F .
- For algorithms having different t_k points, AUC uses interpolation to create comparable $F(t)$ curves across a common time range 0 to T_{\max} , and thus giving a fair comparison without needing synchronizing the curve.
- By integrating $F(t)$ over time, AUC summarizes the entire performance from start to T_{\max} , not just a single point
- AUC is robust to early stopping: for algorithm stops early, AUC can handle it by the extrapolation. This ensures all algorithms are evaluated over the same time window.

Sparsity measure: We also report the sparsity (expressed as percentage) of the output \mathbf{H}_{Last} using the formula $\text{nnz}(\mathbf{H}_{\text{last}} > 10^{-9})/nr\%$. That is, we take entries in $\text{nnz}(\mathbf{H}_{\text{last}})$ below 10^{-9} as zero, and count the percentage of zeros in \mathbf{H}_{last} with respect to the total number of entries rn .

3.4 Results and Discussion

In this section, we report the results on three different-sized dataset, with the same sparsity level for \mathbf{H} (set as 0.6), and 3 different noise levels $\sigma = 0, 0.1, 0.3$. The datasets we refer to are considered as: i) small size data, $(m, n, r) = (20, 100, 3)$; ii) medium size data, $(m, n, r) = (50, 1000, 3)$; iii) high size data, $(m, n, r) = (100, 10000, 3)$. Tables 2,3,4 reports the results on the three datasets, according to the setting and metrics detailed before.

Table 2: The final function value obtained by the algorithms on small size dataset $(m, n, r, s, k_{\text{max}}, T_{\text{max}}) = (20, 100, 3, 0.6, 10^6, 5)$: Average error, standard deviation, rankings, and sparsity among the 100 runs (100 datasets).

Method	mean \pm std of F_{Last}	ranking in 100 runs	median sparsity% of \mathbf{H}_{Last}
No noise $\sigma = 0$			
EMU-proj	152.461 \pm 24.988	(13, 0, 8, 79)	40.667
SMU-L1	150.303 \pm 27.674	(4, 1, 80, 15)	73.167
RMU	141.528 \pm 25.39	(27, 56, 11, 6)	63.833
RCG	140.047 \pm 25.428	(56, 43, 1, 0)	100.00
low noise $\sigma = 0.1$			
EMU-proj	172.911 \pm 25.445	(20, 0, 9, 71)	41.009
SMU-L1	177.290 \pm 27.487	(6, 0, 75, 19)	83.333
RMU	164.662 \pm 25.855	(53, 21, 16, 10)	62.667
RCG	163.275 \pm 26.078	(21, 79, 0, 0)	100.000
high noise $\sigma = 0.3$			
EMU-proj	235.001 \pm 28.449	(46, 0, 22, 32)	39.333
SMU-L1	257.266 \pm 34.775	(6, 0, 56, 38)	88.000
RMU	232.738 \pm 31.296	(45, 3, 22, 30)	57.000
RCG	232.232 \pm 31.951	(3, 97, 0, 0)	100.000

Based on the ranking values shown in the tables, it can be observed that RCG performs better on small datasets, while RMU excels with larger datasets. The proposed method is faster and more cost-efficient due to lower computational overhead per iteration. Therefore, RMU can be considered a suitable alternative for large-scale problems when extremely high accuracy is not essential.

For the sparsity, we firstly remark that, for RCG, the median sparsity% is always 100%. This is because after say 39289 iterations, the smallest entry of \mathbf{H}_{Last} produced by RCG has a magnitude of 5.3×10^{-8} , not reaching 10^{-9} . Regarding the comparison of other methods, we should remark that even when they reach a better sparsity measure or minimization point, these come from heuristic approaches where the normalization is performed a posteriori with a projection step. In fact, although

Table 3: The final function value obtained by the algorithms on medium size dataset $(m, n, r, s, k_{\max}, T_{\max}) = (50, 1000, 3, 0.6, 10^6, 5)$: Average error, standard deviation, rankings, and sparsity among the 100 runs (100 datasets).

Method	mean \pm std of F_{Last}	ranking in 100 runs	median sparsity% of \mathbf{H}_{Last}
No noise $\sigma = 0$			
EMU-proj	4997.577 \pm 371.044	(82, 0, 16, 2)	33.950
SMU-L1	5385.953 \pm 408.194	(5, 0, 81, 14)	69.834
RMU	5128.349 \pm 369.939	(10, 3, 3, 84)	59.117
RCG	5171.701 \pm 391.186	(3, 97, 0, 0)	99.967
low noise $\sigma = 0.1$			
EMU-proj	5644.770 \pm 424.276	(86, 0, 14, 0)	33.917
SMU-L1	6312.159 \pm 455.600	(4, 0, 86, 10)	77.900
RMU	5843.769 \pm 412.325	(10, 0, 0, 90)	55.767
RCG	5943.416 \pm 431.832	(0, 100, 0, 0)	99.967
high noise $\sigma = 0.3$			
EMU-proj	7696.908 \pm 433.299	(89, 0, 11, 0)	33.833
SMU-L1	9078.844 \pm 561.377	(8, 0, 89, 3)	83.433
RMU	8018.144 \pm 499.013	(3, 0, 0, 97)	50.167
RCG	8327.873 \pm 540.228	(0, 100, 0, 0)	100.000

Table 4: The final function value obtained by the algorithms on high size dataset $(m, n, r, s, k_{\max}, T_{\max}) = (100, 10000, 3, 0.6, 10^6, 5)$: Average error, standard deviation, rankings, and sparsity among the 100 runs (100 datasets).

Method	mean \pm std of F_{Last}	ranking in 100 runs	median sparsity% of \mathbf{H}_{Last}
No noise $\sigma = 0$			
EMU-proj	133414.794 \pm 5835.101	(99, 0, 1, 0)	33.457
SMU-L1	153855.389 \pm 7467.903	(1, 0, 99, 0)	67.687
RMU	142953.115 \pm 6565.514	(0, 99, 0, 1)	50.773
RCG	155081.249 \pm 8132.666	(0, 1, 0, 99)	99.993
low noise $\sigma = 0.1$			
EMU-proj	151988.784 \pm 6317.544	(98, 0, 2, 0)	33.457
SMU-L1	179816.744 \pm 8255.746	(2, 0, 98, 0)	70.720
RMU	161917.731 \pm 6982.220	(0, 98, 0, 2)	47.598
RCG	179762.518 \pm 8911.506	(0, 2, 0, 98)	99.993
high noise $\sigma = 0.3$			
EMU-proj	205028.436 \pm 8094.901	(95, 0, 5, 0)	33.477
SMU-L1	251804.877 \pm 10254.644	(5, 0, 95, 0)	76.927
RMU	213833.682 \pm 8784.789	(0, 73, 0, 27)	40.875
RCG	238907.396 \pm 9286.034	(0, 27, 0, 73)	99.990

both methods preserve the normalization of the columns of \mathbf{H} , RMU achieves a better minimization of the objective function, while also yielding improved sparsity and integrating the normalization directly into the optimization process without requiring additional computational steps.

4 Conclusion

In this paper, we have proposed a novel manifold optimization method to solve low-rank problems with sparse simplex constraints by leveraging oblique rotation manifolds. Our approach ensures that the nonnegativity, sparsity, and sum-to-one conditions are preserved throughout the optimization process while maintaining the convergence properties of Riemannian gradient descent.

Experiments on synthetic datasets have demonstrated the effectiveness of the proposed method compared to standard Euclidean and Riemannian optimization techniques. Specifically, we performed comparable and sometimes better solutions faster than the considered methods. Moreover, comparing to the Riemannian approach, the proposed RMU has no need to compute vector transport also nor face with Wolfe line search limits, making RMU appealing for large-scale problems. In fact, our approach exhibits improved convergence behavior, numerical stability, and the ability to better exploit the underlying low-rank structure of the problem, particularly for high-dimensional problems. These advantages make it particularly suitable for applications where structured low-rank solutions with simplex constraints are essential, such as in signal processing, machine learning, and computational biology.

Future work will focus on extending the method to explore adaptive strategies for manifold parameterization and investigating its applicability to real-world datasets in diverse domains.

Acknowledgements. F.E. is member of the Gruppo Nazionale Calcolo Scientifico - Istituto Nazionale di Alta Matematica (GNCS - INdAM).

F.E. wants to thank Prof. Del Buono from University of Bary for the useful scientific discussion.

Declarations

- **Funding:** This work was supported by INdAM - GNCS Project *Ottimizzazione e Algebra Lineare Randomizzata* (CUP E53C24001950001 to F.E.), and Piano Nazionale di Ripresa e Resilienza (PNRR), Missione 4 “Istruzione e Ricerca”- Componente C2 Investimento 1.1, “Fondo per il Programma Nazionale di Ricerca e Progetti di Rilevante Interesse Nazionale”, Progetto PRIN-2022 PNRR, P2022BLN38, *Computational approaches for the integration of multi-omics data* (CUP H53D23008870001, to F.E.).
- **Conflict of interest/Competing interests** (check journal-specific guidelines for which heading to use): The authors declare no competing interests.
- **Ethics approval and consent to participate:** Not applicable.
- **Consent for publication:** All authors give the consent for publication.
- **Data availability :** data are synthetically generated.
- **Materials availability:** Not applicable.
- **Code availability:** The code will be accessible on <https://github.com/flaespo>.
- **Author contribution:** All authors contribute equally to the work.

References

- [1] Gillis, N.: Nonnegative Matrix Factorization. Society for Industrial and Applied Mathematics, Philadelphia, PA (2020). <https://doi.org/10.1137/1.9781611976410>
- [2] Udell, M., Townsend, A.: Why Are Big Data Matrices Approximately Low Rank? SIAM Journal on Mathematics of Data Science **1**(1), 144–160 (2019) <https://doi.org/10.1137/18M1183480>
- [3] Brunet, J.-P., Tamayo, P., Golub, T.R., Mesirov, J.P.: Metagenes and molecular pattern discovery using matrix factorization. Proceedings of the National Academy of Sciences **101**(12), 4164–4169 (2004) <https://doi.org/10.1073/pnas.0308531101>
- [4] Xu, Z., Chang, X., Xu, F., Zhang, H.: $l_{1/2}$ regularization: A Thresholding Representation Theory and a Fast Solver. IEEE Transactions on Neural Networks and Learning Systems **23**(7), 1013–1027 (2012) <https://doi.org/10.1109/TNNLS.2012.2197412>
- [5] Esposito, F., Ang, A.: Chordal-NMF with Riemannian Multiplicative Update (2024) [arXiv:2405.12823](https://arxiv.org/abs/2405.12823)
- [6] Qian, Y., Jia, S., Zhou, J., Robles-Kelly, A.: Hyperspectral Unmixing via $L_{1/2}$ Sparsity-Constrained Nonnegative Matrix Factorization. IEEE Transactions on Geoscience and Remote Sensing **49**(11), 4282–4297 (2011) <https://doi.org/10.1109/TGRS.2011.2144605>
- [7] Guo, Z., Min, A., Yang, B., Chen, J., Li, H., Gao, J.: A Sparse Oblique-Manifold Nonnegative Matrix Factorization for Hyperspectral Unmixing. IEEE Transactions on Geoscience and Remote Sensing **60**, 1–13 (2022) <https://doi.org/10.1109/TGRS.2021.3082255>
- [8] Ang, A., Ma, J., Liu, N., Huang, K., Wang, Y.: Fast Projection onto the Capped Simplex with Applications to Sparse Regression in Bioinformatics. In: Proceedings of the 35th International Conference on Neural Information Processing Systems. NIPS '21. Curran Associates Inc., Red Hook, NY, USA (2021)
- [9] Absil, P.-A., Mahony, R., Sepulchre, R.: Optimization Algorithms on Matrix Manifolds, p. 224. Princeton University Press, Princeton, NJ (2008)
- [10] Yin, P., Lou, Y., He, Q., Xin, J.: Minimization of ℓ_{1-2} for Compressed Sensing. SIAM Journal on Scientific Computing **37**(1), 536–563 (2015) <https://doi.org/10.1137/140952363>
- [11] Ahmadi, A.A., Olshevsky, A., Parrilo, P.A., Tsitsiklis, J.N.: NP-hardness of Deciding Convexity of Quartic Polynomials and Related Problems. Mathematical

programming **137**, 453–476 (2013) <https://doi.org/10.1007/s10107-011-0499-2>

- [12] Boumal, N.: An Introduction to Optimization on Smooth Manifolds. Cambridge University Press, Cambridge, UK (2023). <https://doi.org/10.1017/9781009166164>
- [13] Beck, A.: First-Order Methods in Optimization. Society for Industrial and Applied Mathematics, Philadelphia, PA (2017). <https://doi.org/10.1137/1.9781611974997>
- [14] Hoyer, P.O.: Non-negative sparse coding. In: Proceedings of the 12th IEEE Workshop on Neural Networks for Signal Processing, pp. 557–565 (2002). <https://doi.org/10.1109/NNSP.2002.1030067> . IEEE
- [15] Eggert, J., Korner, E.: Sparse coding and NMF. In: 2004 IEEE International Joint Conference on Neural Networks (IEEE Cat. No. 04CH37541), vol. 4, pp. 2529–2533 (2004). <https://doi.org/10.1109/IJCNN.2004.1381036> . IEEE
- [16] Boutsidis, C., Galloopoulos, E.: SVD based initialization: A head start for non-negative matrix factorization. Pattern recognition **41**(4), 1350–1362 (2008) <https://doi.org/10.1016/j.patcog.2007.09.010>